Hydraulics Research
Wallingford

A BUOYANT SURFACE JET IN A STRONG CROSS-FLOW

Report No SR 68
October 1985

Registered Office: Hydraulics Research Limited,
Wallingford, Oxfordshire OX10 8BA.
Telephone: 0491 35381. Telex: 848552

ABSTRACT

This report deals with an investigation of the near-field behaviour of a buoyant rectangular surface jet discharging normally onto a strong cross-flow. Surface buoyant jets are frequently found in nature and man's projects. They arise from a combination of momentum and buoyancy injected onto the free surface of the receiving body of water in motion or at rest.

A great deal of work, both experimentally and theoretically, has been undertaken to understand and to model surface buoyant jets in stagnant water, allowing reasonably good predictions of the spread and dilution of wastes. These predictions are inaccurate when the ambient cross-flow is strong. It is widely believed that a large dilution of pollutants will occur near the outfall, and that the mixing process depends very much on the flow turbulence, and that the outfall Reynolds number plays an important part in the dilution of a buoyant jet, but few measurements of turbulence have been reported so far.

With this in mind a physical model study of a buoyant rectangular surface jet discharging onto a strong cross-flow has been conducted, with a ratio of the buoyant jet velocity to that of the cross-flow in the order of unity. Warm water at about 73°C was discharged into a cold water cross-flow. Mean temperature and its fluctuations together with mean velocity were measured at three elevations at various sections downstream from the outfall. From the measured data, isotherms in both horizontal and vertical planes, together with later mean velocity profiles were determined. The jet-axis, as the locus of maximum temperature, and the dilution factor along the axis were determined at three elevations. Turbulence parameters and warm water flux were measured at one section.

ACKNOWLEDGEMENTS

This report describes work carried out under contract No PECD 7/7/050, funded by the Department of the Environment. The DOE nominated officer was Mr C E Wright. The work was carried out by Dr H O Anwar in the Tidal Engineering Department of Hydraulics Research. Mr M F C Thorn, Head of the Tidal Engineering, was the company's nominated project officer.

CONTENTS

PLATES

1 INTRODUCTION

The quality standard of water in lakes, river and coastal waters is often constrainéd by the release of pollutants such as heat, chemically charged effluents and fine suspensions. Thus it becomes necessary to predict the pollutant concentration at specified distances from the source of release: such a prediction is not straight forward.

A large mixing process of pollutants with ambient water occurs in the vicinity of the release point[3,8], hence the calculation of pollutant concentrations depends very much on the type of discharges, among which a surface discharge onto a cross-flow has the least permanent ecological impact in comparison with the other types.

The great difficulty in obtaining reliable field data, and also less than completely satisfactory predictive capability of the existing theorical and numerical models, have motivated the Hydraulics Research Ltd to undertake a laboratory investigation of a rectangular buoyant jet entering normally a uniform cross-flow at a relatively high velocity. In most existing laboratory studies either the buoyant jet velocity or that of the cross-flow is low, limiting the value of laboratory data for predicting the behaviour of full scale surface plumes with Reynolds numbers one or two orders of magnitude higher.

Whilst it has commonly been assumed that the turbulence in a buoyant jet, and thus the mixing process, relatively insensitive to the Reynolds number above a critical value[3,4], extrapolation of the laboratory data beyond the range of the tested Reynold numbers would be only acceptable, if, over that range, there is a clear evidence that the surface buoyant jet behaviour is independent of this criterion[7]. On the other hand, Kuhlman[8,9] has shown clearly that the trajectory and the spread of a buoyant surface jet in a cross-flow depend strongly on the Reynolds number of the buoyant jet, mainly due to the appearance of kidney-shape vortices in the spreading jet[5,8]. The development of these vortices depends on the jet Reynolds number, and also on the ratio of the ambient velocity to that of the buoyant jet[1,2,6]. The present experimental study was designed to measure the mean temperatures and temperature fluctuations, together with velocities, in the mean jet-flow direction at various elevations across the spreading buoyant jet in a strong cross-flow. Warm water of 73°C was discharged from a rectangular open channel onto a two-dimensional boundary layer cross-flow of cold water, producing a temperature rise of 58°C. The Reynolds numbers of the buoyant jet and that of the cross-flow, both based on the each flow depth, were 11×10^4 and 7×10^4 respectively. The velocity ratio of the cross-flow to that of the jet was 0.90, and the densimetric Froude number $F_r = 1.7$.

From the measured data, horizontal isotherms were determined at three elevations and vertical isotherms for various sections downstream from the outfall. Profiles of turbulence intensities for temperature fluctuations, mean temperature and mean velocity profiles in the flow direction were determined at various sections perpendicular to the jet-axis at a depth of 0.02, 0.05 and 0.1m below the free surface. At one section, velocity and it fluctuation in the mean flow direction, together with the temperature and its fluctuation, were measured simultaneously at 50mm depth below the surface. The turbulence length scales, flatness factor and the turbulent warm water flux were evaluated from the velocity, and also the temperature fluctuations. The results indicate that the flow of the buoyant jet is highly three-dimensional, and the measured profiles are not geometrically similar at various sections and elevations. Hence, measured data were normalised using the warm water velocity and its depth at the outfall exit, together with the temperature difference between the jet and the cold water of the cross-flow as scale quantities.

The objective of the present study is to determine the terms required for calculating the spread of a buoyant surface jet in a strong cross-flow, and it is hoped that the measured data will provide a better understanding of the complex flow structure and the effect of buoyancy on turbulence.

2 EXPERIMENTAL SET UP

The experiments were conducted in two especially designed flumes. The cross-flow flume, representing the ambient condition, was 3.66m wide, 0.45m deep and 40m long. In the flume entrance there were baffles and a 0.65m long honeycomb (see Plate 1). These, together with two large diffuser outlets in the flume entry, provided a uniform flow of cold water in the test section; the variation of velocity across the flume 15m downstream from the entrance was found to be not greater than 2% for a mean velocity varying between 0.2 and 0.30ms^{-1} without a trend in the lateral direction. The cold water in the flume was circulated by three centrifugal pumps, capable of producing ambient currents of up to 0.30 ms^{-1}. The water level in the flume was controlled by a series of needle weirs (see Plate 2), blocking part of the flow area at the exit to obtain the required water depth. This arrangement provided flow without any stagnation, the occurrence of this in the ambient current near the flume exit could affect the measured data. Hot water, representing the pollutant, was discharged from a rectangular channel outfall 3.8 long, 0.25m wide 0.30m deep with invert 0.15m above the bed of the cross-flow flume and projecting 0.30m into it with transition walls upstream and downstream to prevent flow separation (see Plate 2). A series of screens were used in the entrance of the channel outfall to obtain a uniform flow, the effectiveness of which was confirmed experimentally. With channel outfall constructed in wood it was found that heat losses through the rigid channel boundaries were small.

Hot water at about 73°C was supplied to the outfall from a tank with a capacity of $28m^3$. This tank, heavily insulated to minimize heat loss, was equipped with a 36kw immersion heater, which together with an auxilliary 3kw immersion heater brought into operation during the experimental runs, were controlled by a thermostat to give the required temperature. The water in the tank was constantly circulated by a pump in order to obtain a homogeneous warm water supply, which, in turn, was pumped to the channel outfall via an insulated pipe. The temperature loss between the tank and the outfall was found to be less than 2°C.

3 TEMPERATURE

The temperature and its fluctuation in the buoyant jet were examined by means of thermistors with time constants in the order of 0.25s when immersed in water. The variation of temperature in the spreading jet was large, hence it was not possible to linearise the thermister's output, so electronic circuitry was designed to produce non-linear outputs over the temperature range varying between zero and 70°C. A maximum of 20 thermistors could be used at a time and their signals were recorded on magnetic tape. Using a data-logger the temperature and its fluctuation at a point could be determined from calibration curves in the form of forth order polynomials fitted to the measured data by a least square method. The resolution was found to be in the order of 0.1°C.

During the experimental runs the mean temperature in the channel outfall and the background temperature in the cross-flow flume were measured using digital thermometers, their readings gave an immediate check of any temperature changes which may have occurred during the run, but it was found that the temperature in the channel outfall remained constant. The combined discharge of water from the cross-flow flume flowed into a large reservoir to which cold water was added continuously during the measurement; the experiment was stopped when the background temperature increased 0.5°C.

The mean velocity profiles in the lateral directions were measured at z = 0.02, 0.05 and 0.1m using nine 10mm diameter miniature propeller current meters, their outputs were recorded on a magnetic tape. Each current meter cold be rotated about its vertical stem in order to measure the true velocity in the mean flow direction, as became necessary in the deflected region of the jet. Since high temperatures affected the miniature propeller bearings, the velocity in the channel outfall was measured with a Ott current meter of 25mm diameter.

All thermistors and miniature propeller current meters were mounted on an aluminium frame spanning the cross-flow flume (see Plate 2). A mechanism built into the frame allowed positioning of thermistors and current meters at various elevations in the buoyant jet. The entire assembly was mounted on a carriage so that it could be moved manually in the mean cross-flow direction to any desired section of the flume.

The sampling time for taking temperature at each point was approximately 150 seconds. The variation of the mean temperature, and its fluctuation within the duration of sampling period, are shown in Fig 1, indicating that the measured data remained almost unchanged when the sampling time exceeded 100 seconds. The rms and the mean values of the temperature were evaluated according to the following expression:

$$T = \frac{1}{N}\sum_{1}^{N} t_n, \quad (\overline{t^2})^{\frac{1}{2}} = \left[\frac{1}{N}\sum_{n=1}^{N} \overline{(t_n - T)^2}\right]^{\frac{1}{2}} \tag{1}$$

where t_n is the instantaneous temperature.

4 MEASUREMENTS

4.1 Velocity

It was necessary to determine the mean velocity profile in the cross-flow flume near the channel outfall. The mean velocity profile for the free stream velocity $U_m = 0.3ms^{-1}$ was measured at the flume centreline over a hydraulically smooth bed at 2m upstream from the outfall. The result showed that the thickness of the boundary layers was approximately 0.1m for a total water depth H = 0.32m. In order to obtain a fully developed boundary layer flow of the thickness H the flow was tripped using a commercially produced aluminium expanding mesh, covering the width of the flume for a length of 5m. The expanded mesh was fixed to the flume floor immediately downstream from the honeycomb baffle visible in Plate 1. With this arrangement a fully developed turbulent boundary layer upstream from the channel outfall was obtained, and a logarithmic profile expressed in the following form has been fitted to the measured profile by least squares sense, ie:

$$\frac{U}{U_*} = \frac{1}{K}\frac{U_* z}{\nu} + B \tag{2}$$

where U is the local mean velocity at elevation z and U_* is the friction velocity (= $\sqrt{\tau_o/\rho}$, where τ_o is the bed shear stress and ρ is the mass density of the cold water). In equation (2) B is a constant and the experimental result revealed that B = 8.5; k = 0.4 is the Karman constant. The measured profile is presented non-dimensionally in Fig 2. Similarly the velocity profile was measured in the channel outfall and the result in non-dimensional form is also shown in Fig 4 with B = 8.14 and k = 0.4.

4.2 Temperature

Temperatures were measured in the vertical (y - z) plane (see Fig 3) at various sections x = 0.0m to 5m with increments of 0.25m downstream from the outfall. The measurements were made at z = 0.02, 0.05 and 0.1m below the free surface.

4.3 Results

From the measured temperature data, vertical isotherms in the vertical (y - z) plane for various distances x were determined and the results for x = 0.0, up to x = 5m are shown in Figs 4 (a - c) and Fig 5 (a - c), indicating that the buoyant jet widens as the downstream distance x increases. These figures further show that the maximum isotherm near the free surface moves towards the outer boundary of the cross-flow flume with increasing distance x. These results agree reasonably well with those obtained by Kuhlman[8]. Figs 4 (a-c) indicate that the buoyant jet thickens immediately downstream from the outfall, entraining the ambient cold water. The mixing in this region, ie between x = 0 and x = 0.5m, is dominated mainly by the jet-flow due to the fact that U_j is larger than the ambient velocity U_a ($R = \frac{U_a}{U_j} = \frac{0.28}{0.31}$ (ms^{-1}) = 0.9). Downstream from x = 0.5m (see Figs 5 (a - c)) the buoyant jet became thinner and wider incomparison to those shown in Figs 4 (a - c). This implies that buoyancy effect prohibits the vertical mixing, but not the lateral spread which will be discussed later. Figs 4 and 5 further show an inner region containing warm water with an almost constant excess temperature above that of the cross-flow. The flow in this inner region behaved much like that in the wake, with a reverse-flow near the inner wall of the cross-flow flume. The movement is complex, and no attempt was made to explore the flow structure in the wake-type region, but the results of measurements to be shown later are interesting.

From the measured temperatures horizontal isotherm contours (in the x-y plane (see Fig 3)) were constructed for z = 0.02, 0.05 and 0.1m and the results are presented in Figs 6 (a - c). In these figures are shown the buoyant jet-axis, defined as the locus of points at which the temperature rise above the cross-flow temperature is a maximum. Figs 6 (a - c) show that the jet axis moved towards the inner wall of the cross-flow flume and that the jet became narrower as z increased. This is due to the mutual deflections of the jet and the cross-flow. The flow of the ambient cold water beneath the jet maked the buoyant jet flow in the bend region highly three dimensional, which will be shown later. In Fig 5 (a - c) are also shown dashed lines which were obtained by joining points at which the temperatures rise in the wake-type region is a maximum. The temperature here and its variation along the dashed axis is much smaller than that along the main jet-axis. The dashed axes eventually jointed the inner wall of the cross-flow flume at a downstream distance x = 7m, where the wake-type region terminated. Figs 6 (a - b) show that the dashed axes for maximum temperature start at x = 0.5m. It is believed that the start and the extent of the dashed axis depends strongly on the velocity ratio R.

4.4 Lateral Velocity Profiles

From the velocities, measured in the mean flow direction at z = 0.02, 0.05 and 0.1m, the lateral velocity profiles in a plane perpendicular to the jet axis at z = 50mm (see Fig 6b) were determined and the results are given in Figs 7 and 8, together with the profiles for the mean temperature and for the turbulence intensity of the temperature fluctuations.

In these figures $\Delta\theta_j = T_j - T_a$ and $\Delta\theta = T - T_a$ (see also Fig 3). It should be noted that the velocity profiles at z = 0.02m and z = 0.1m were measured in the mean flow direction, but at planes which were perpendicular to the jet axis z = 0.05m (see Figs 4 and 5) in order to facilitate the experimental procedure. Figs 7 and 8 show that the mean temperature profiles are severely skewed, and it was not possible to present them by a single non-dimensional curve. As mentioned previously the jet becomes narrower with increasing z. Figs 7 and 8 show the double peaks in the mean temperature profiles. The locus of these double peaks were the jet axis and the wake axis shown in Figs 6 (a - c). Furthermore Figs 7 and 8 exhibit the existence of maxima in the turbulence intensities profiles of temperature which occur where the mean temperature gradients are maxima as it is to be expected. The turbulence intensity $\frac{\theta'}{\Delta\theta_j}$ approached a value in the order of 0.4 in the wake-type zone. It is interesting to note that at the outer edge of the jet where $\Delta\theta \simeq 0$ the turbulence intensity is not zero, indicating that the outer edge is intermittent, which will be discussed later.

The lateral mean velocity profiles shown in Figs 7 and 8 disclose the existence of double peaks in the mean velocity, occurring generally where the mean temperature are maxima. These set of profiles further show that the mean velocity increases towards the outer edge, becoming larger than that of the ambient cross-flow, ie $R > 1$, before falling to the cross-flow velocity U_a. The overshoot velocity, occurring over the outer edge region, indicates that there is an increase in the entrainment of the ambient cold water into the buoyant jet, in agreement with the continuity equations[2].

5 TURBULENT PARAMETERS

In Figs 7 and 8 are shown lateral distributions of the turbulence intensity of temperature fluctuations $\theta'/\Delta\theta_j$ and those of the mean temperature rises $\Delta\theta/\Delta\theta_j$. The turbulence intensity profiles generally have two peaks, occurring where the gradient of the lateral temperature rise $\Delta\theta$ is the maximum. Figs 7 and 8 further show the existence of turbulence intensities near the outer edge region, implying that a great deal of mixing occurs between the warm water in the jet and the cold water of the cross-flow, as may be seen in Plate 3. In the wake-type region the turbulence intensities are large immediately downstream from the outfall (see Figs 7 (a - b); but decrease downstream (see Figs 8 (b - c). From the results shown in Figs 7 and 8 it can be deduced that the lateral and longitudinal mean temperature gradients are responsible for the production of temperature fluctuations, but this does not mean that the velocity gradients in these directions do not contribute to the temperature fluctuations.

From the measured data it was possible to calculate the turbulent warm water flux $\overline{u'\theta'}$, the flatness factor of temperature fluctuations $F_{\theta'}$ and the turbulent length scale of temperature $L_{\theta'}$ in a section at z = 0.05m shown in Fig 7c. The results are shown in Fig 9. The $\overline{u'\theta'}$ distribution indicates that a large mixing between warm/cold water occurred near the outer edge of the spreading jet. The flatness factor $F_{\theta'}$ indicates that the intermittent nature of temperature field, and is large, especially near the outer edge. As may be seen the temperature length scale $L_{\theta'}$ increases towards the outer edge. It is worth mentioning that the distributions and the magnitude of the flatness factor $F_{u'}$, and the length scale $L_{u'}$ determined from longitudinal velocity fluctuations, were very close to those of $F_{\theta'}$ and $L_{\theta'}$.

6 BUOYANT JET-AXIS

The axis of the buoyant jet, shown in Figs 6 (a - c, is skewed over the bend region, ie $0 < \frac{x}{h_j} < 5$ for z = 0.02m and 0.05m mainly due to the occurrence of the pressure gradient across the jet in the deflected region. It was found that the axes of the jet for z = 0.02 and 0.05m can be described by the following form when $\frac{x}{h_j} > 5$:

$$\frac{y}{h_j} = A\left(\frac{x}{h_j}\right) \qquad (3)$$

which is also applicable for z = 0.1m over the bend region ie $0 < \frac{x}{h_j} < 5$. In Eq (3) A and n are constants, from a least-square linear fit a to the jet-axis the results shown in Table 1 were obtained for constants A and n.

z (mm)	A	n	r
20	2.35	0.5	0.999
50	2.61	0.41	0.999
100	1.61	0.174	0.95

Table 2 Contants of Eq (3)

where r is the correlation coefficient of the fitted curves. It is to be noted that the jet-axis at z = 0.1mm remained almost parallel to the flume wall when $\frac{x}{h_j} > 6$. Table 1 shows that the exponent n is z - dependent; decreasing with increasing depth z. Further measurements are required to determine any effects on the exponent n, of the velocity ratio R, the densimetric Froude number F_r and the outfall

Reynolds number R_e[7,8,9]. The value of n of the present study differs from n = 3/2 and n = 3 found for buoyant surface jets in cross-flows by Kuhlman and Jerka et al[7] respectively. They also found that the exponent n remained unchanged throughout the depth. Furthermore Kuhlman[8] and Jerka et al[7] showed that the velocity ratio R will affect the constant A, by using the length scale R l_o, l_o being the outfall dimensions ie $l_o = (h_j\ b_j)^{\frac{1}{2}}$ (see Fig 3) for normalising x and y. The present results suggest that the R-variation will affect the deflected region of the jet and the cross-flow, and hence the exponent n.

6.1 Dilution on Jet-axis

The dilution along the three axis was defined by the following expression:

$$\frac{T_j - T_a}{T_m - T_a} \qquad (4)$$

where T_m is the temperature along the axes. Expression(4) was calculated from the measured data and the results plotted against y/h_j are shown in Fig 10 for z = 0.02, 0.05 and 0.1m. Fig 10 indicates that the dilution near the surface is small; it increases with increasing z. A large dilution occurred at z = 0.1m mainly due to the entrainment of the ambient cold water of the cross-flow beneath the jet.

7 CONCLUSIONS

The near field behaviour of a buoyant surface jet discharging into a strong cross-flow has been examined with the following results:

1 The mutual deflection of the buoyant surface jet and the cross-flow caused the velocity to rise

along the deflected outer edge of the jet, creating a large entrainment of the ambient cross-flow.

2 In the lee side of the buoyant jet there is a wake-type region with a small return flow near the flume wall. The wake region contained a slow moving body of water with a constant temperature.

3 The lateral distributions of the turbulence intensity of temperature fluctuations showed two peaks and the turbulence intensities are large along the outer edge of the spreading jet.

4 At mid-depth in one cross-section the distributions of turbulent parameters, namely the temperature flatness factor, length scale and the turbulent warm water flux were determined. The maximum of the latter occurred between the jet-axis and the outer-edge of the jet; The flatness factor and length scale increased towards the outer-edge.

5 The shape of the jet axis is depth-dependent and skewed in the bend-region. The asymptotic part of the axis obeys a power law, the exponent being depth-dependent.

6 The dilution along the jet-axis increased with increasing depth.

REFERENCES

1 Andreopoulos J. "Heat transfer measurements in a heated jet-pipe flow issuing into a cold cross stream". Phys Fluids, Vol 26, No 11, November 1983, pp 3201-3210.

2 Andreopoulos J and Rodi W. "Experimental investigation of jets in cross-flow". J Fluid Mech Vol 138, 1984, pp 93-127.

3 Anwar H O. "Appearance of unstable buoyant jet". Proc. ASCE, Vol 98, No HY7, July 1972, pp 1143-1150.

4 Anwar H O. "Behaviour of buoyant jet in calm fluid". Proc. ASCE, Vol 95, NO HY4, July 1969, pp 1289-303.

5 Fearn R and Weston R P. "Vorticity associated with a jet in a cross-flow". AIAA Journal, Vol 12, NO 12, December 1974.

6 Foss J F. "Interaction region of phenomena for the jet in a cross-flow problem". Report SFB 80/E/161, Univ. Karlsruhe, 1980.

7 Jirka G H, Adams E E and Stolzenbach K D. "Buoyant Surface Jet". Proc. ASCE, Vol 107, NO HY11, No 1981, pp 1467-1487.

8 Kuhlman J M. "Effect of Reynolds number on the nearfield region of a buoyant rectangular surface jet in a cross-flow". Final Report, Research for NSF Grants ENG 78-00815 and CME-7800815, Old Dominion Unv. January 1982.

9 Kuhluman J M. "Reynolds number effects on buoyant surface jets". ASCE, J Hydraulic Eng. Vol 110, NO6, June 1984, pp 830-840.

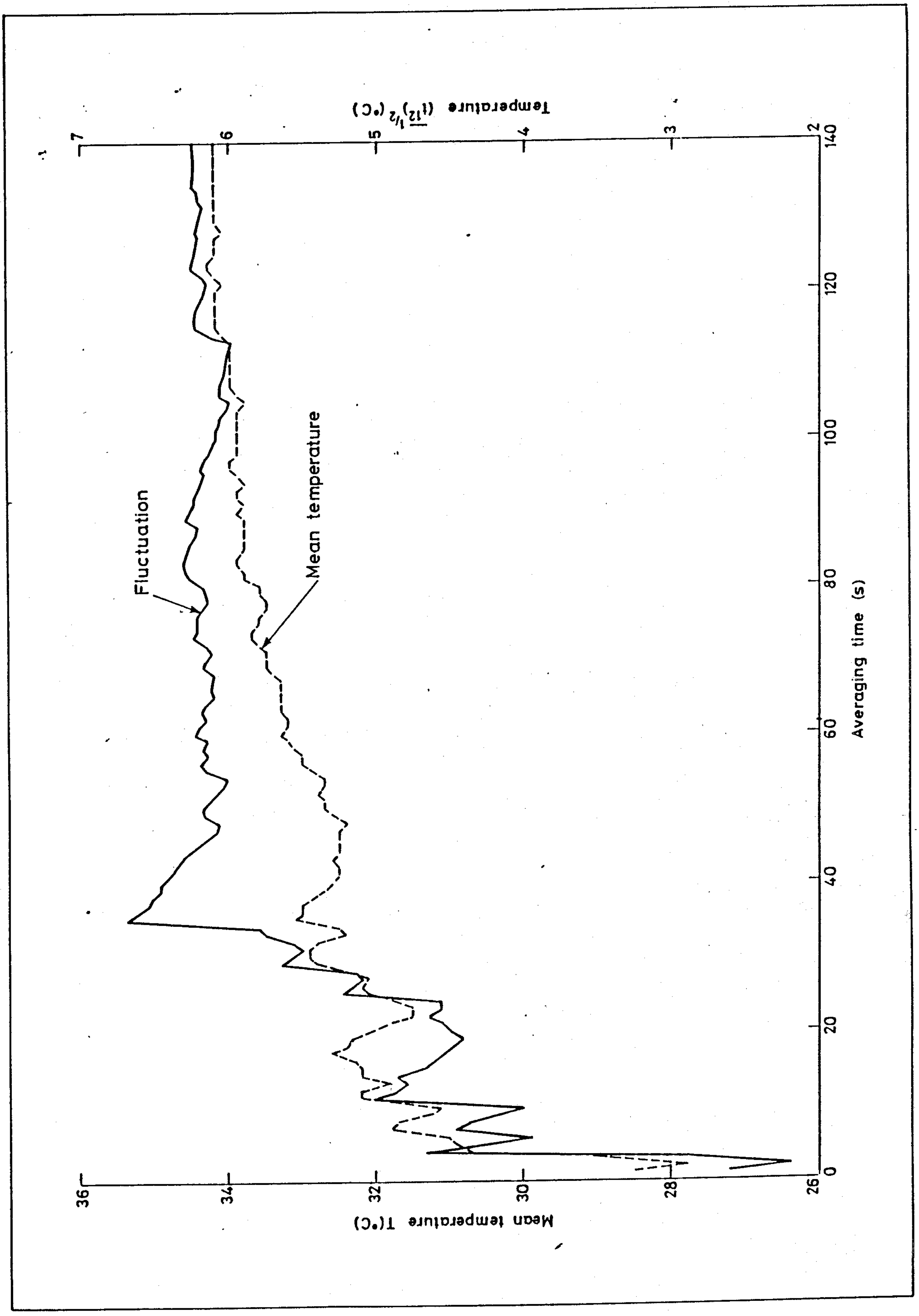

Fig 1 Variation of the mean and rms temperature over the sampling periods

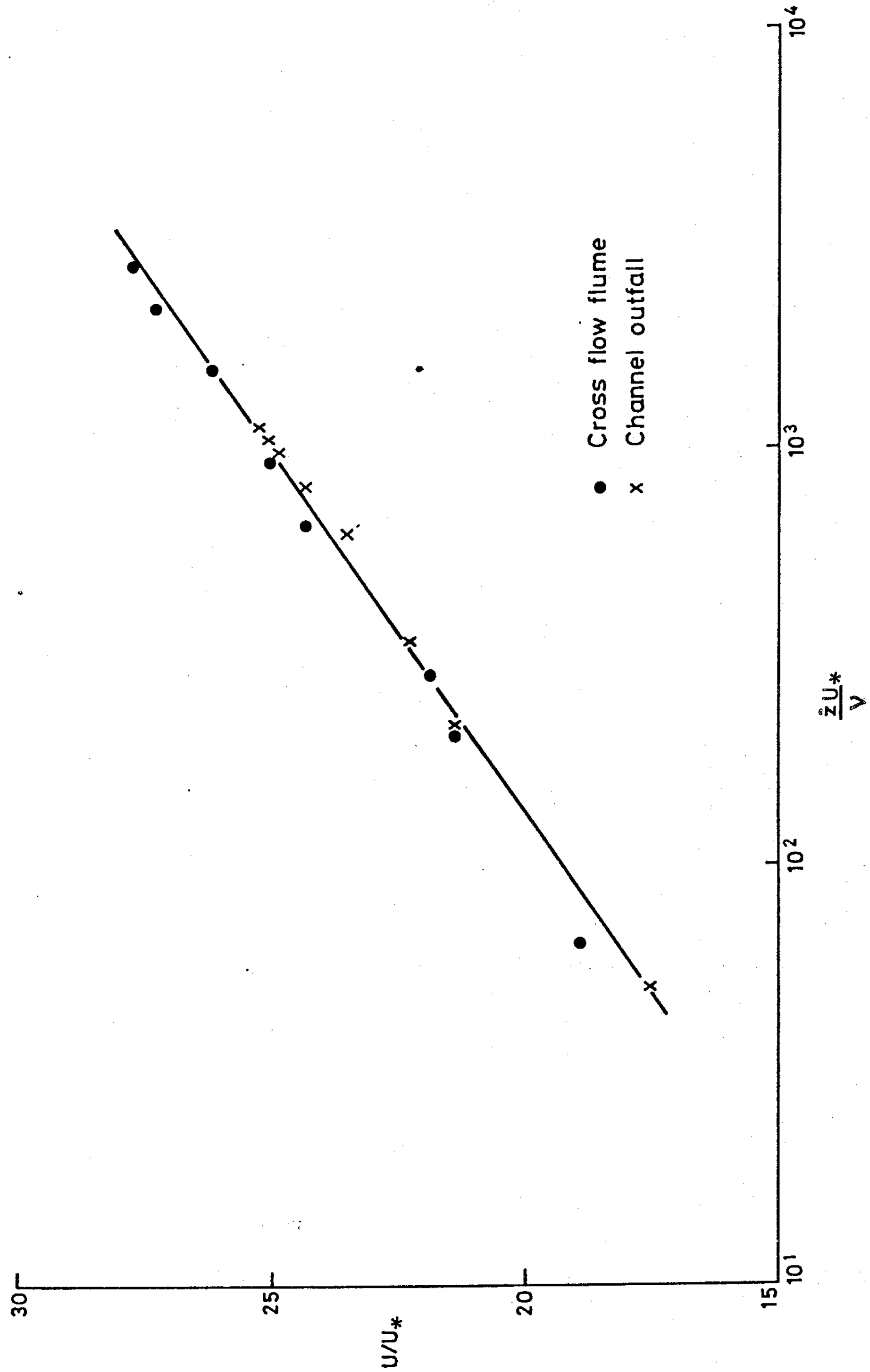

Fig 2 Mean velocity profiles measured at the centre-lines of the cross-flow flume and the channel outfall

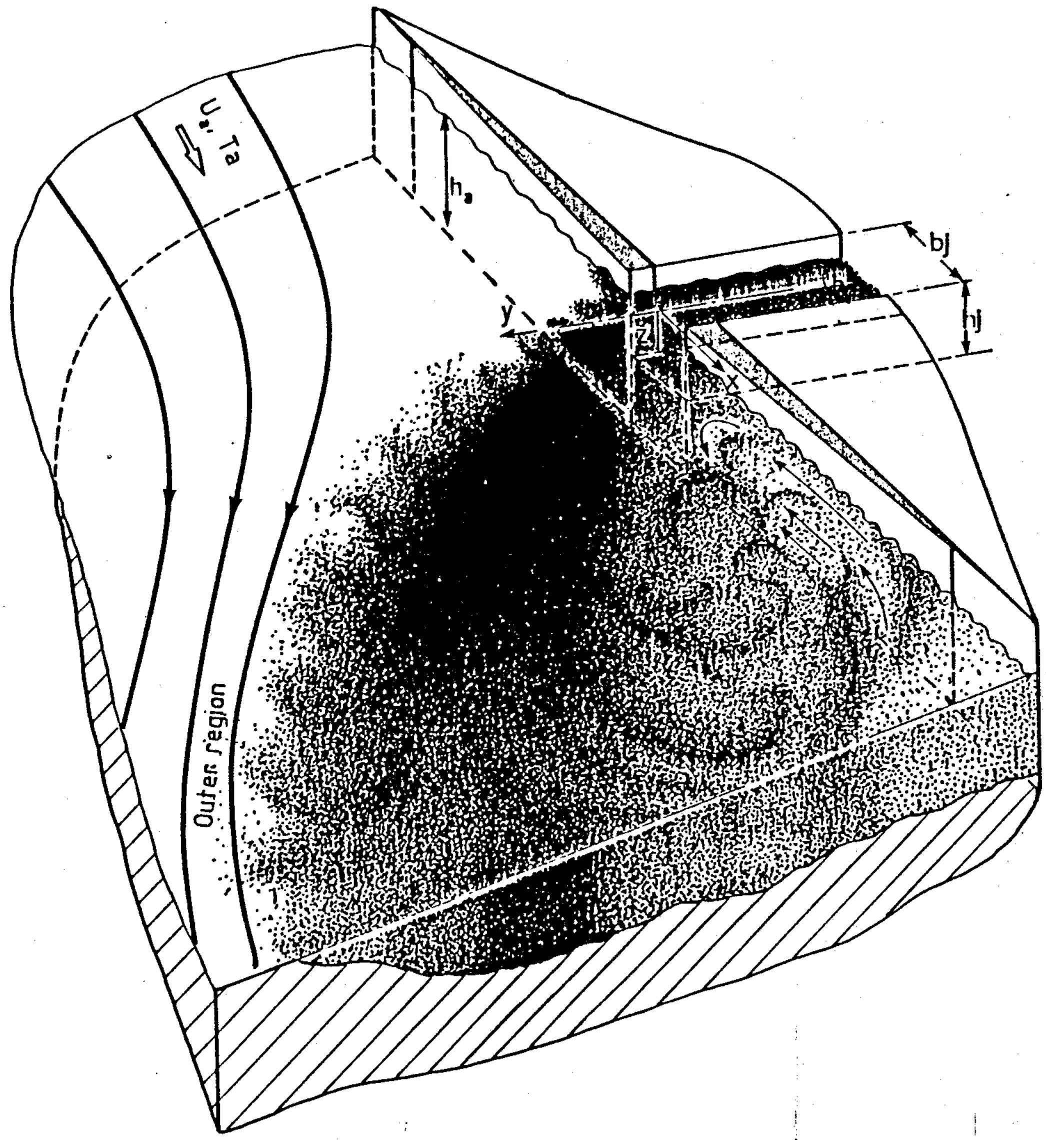

Fig 3 Schematic view with definition of terms of a buoyant jet in a cross-flow

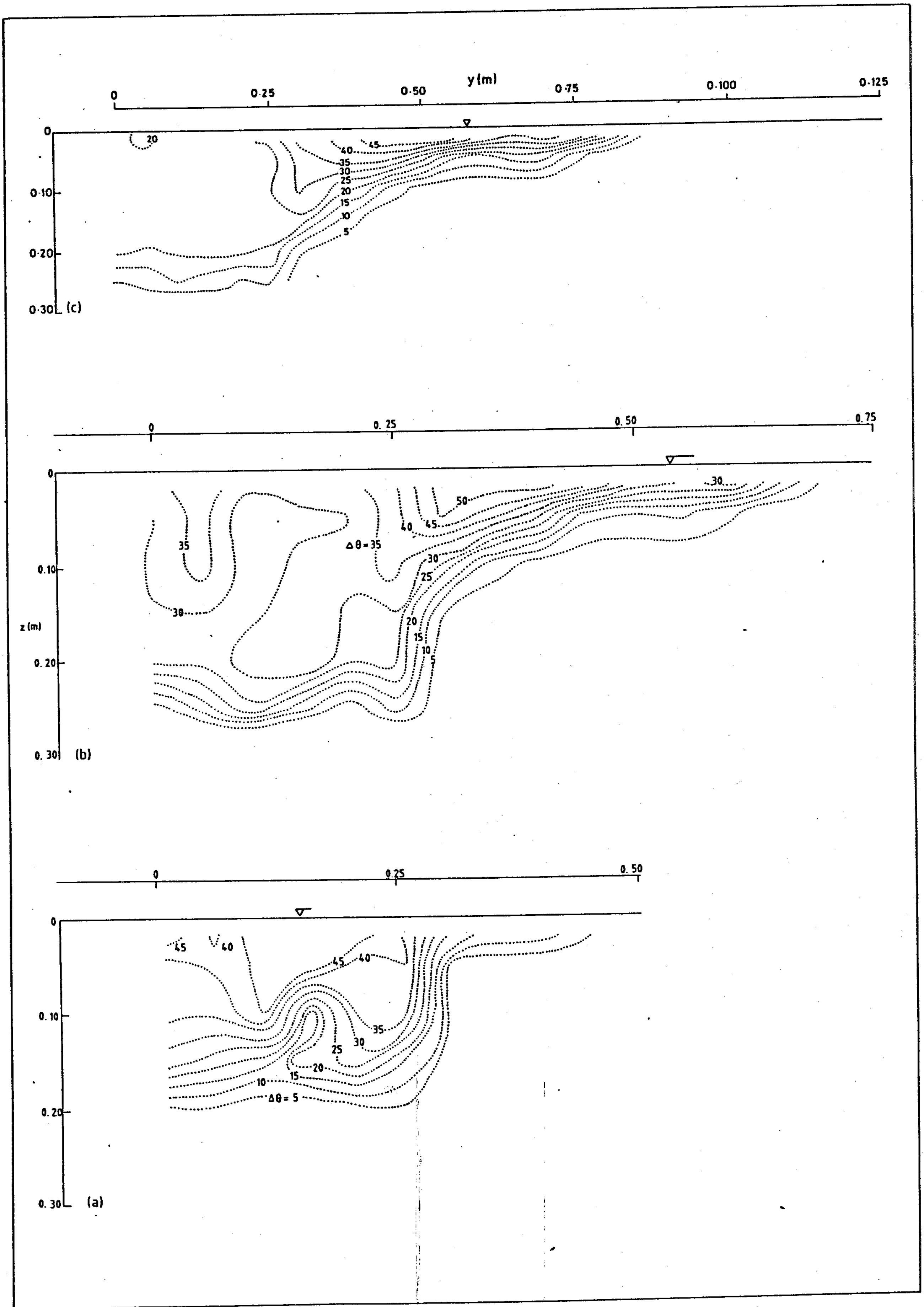

Fig 4 Vertical isotherms at: (a) x = 0.0, (b) x = 0.25m and (c) x = =0.5m, downstream from the outfall (see also Fig 3)

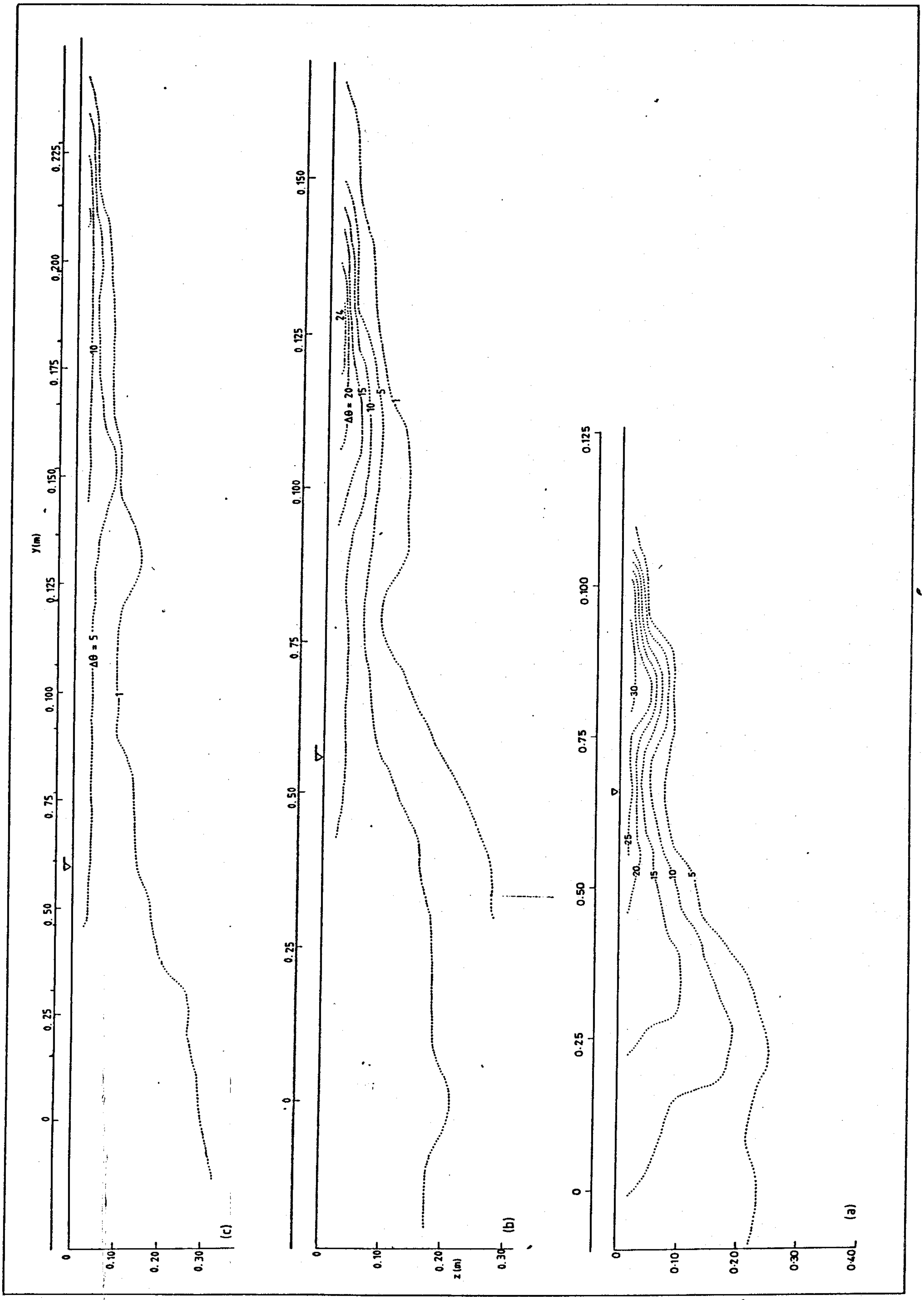

Fig 5 Vertical isotherms: (a) at x = 1m, (b) at x = 2m and (c) at x = 5m downstream from the outfall (see also Fig 3)

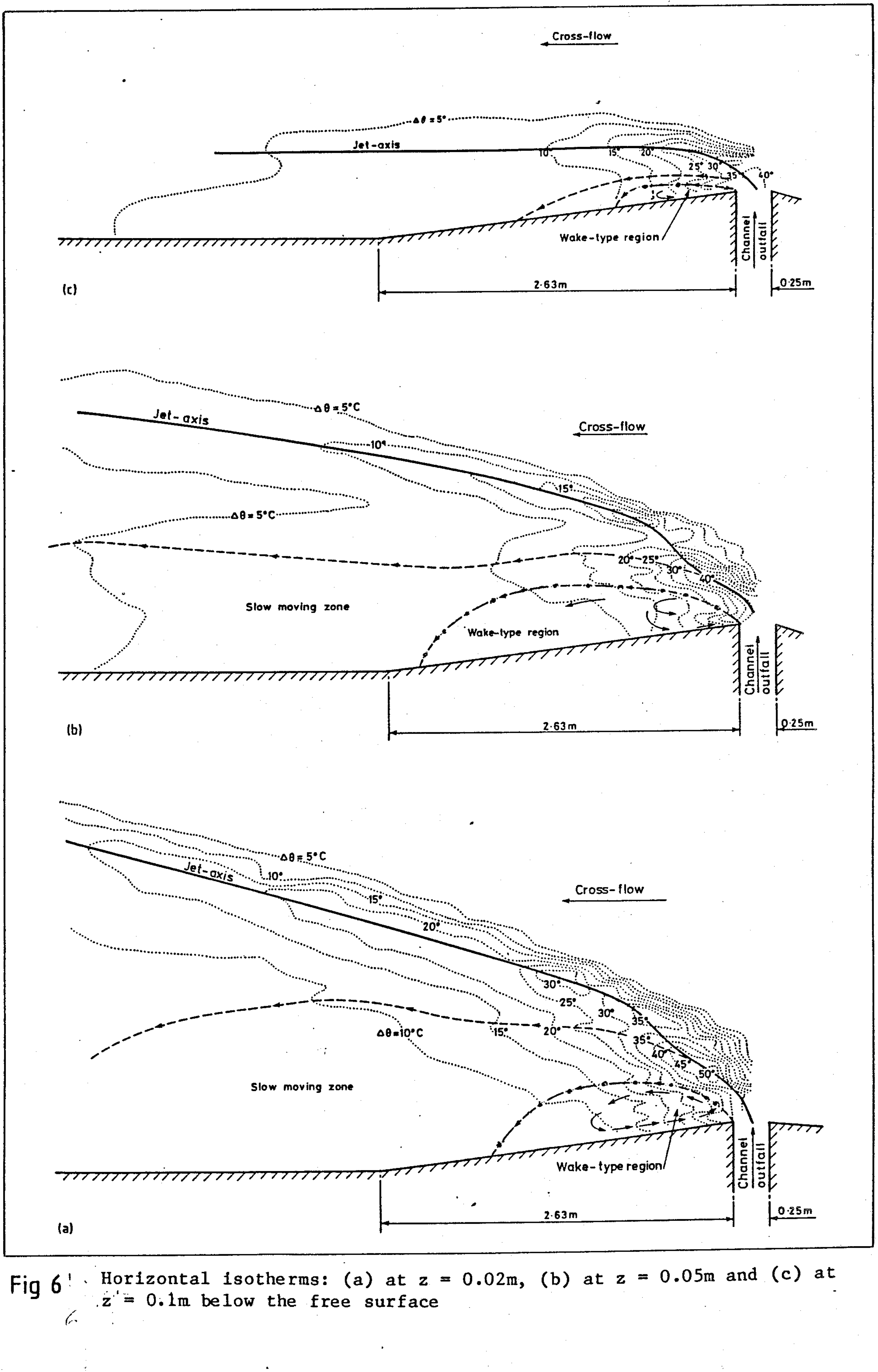

Fig 6 Horizontal isotherms: (a) at z = 0.02m, (b) at z = 0.05m and (c) at z = 0.1m below the free surface

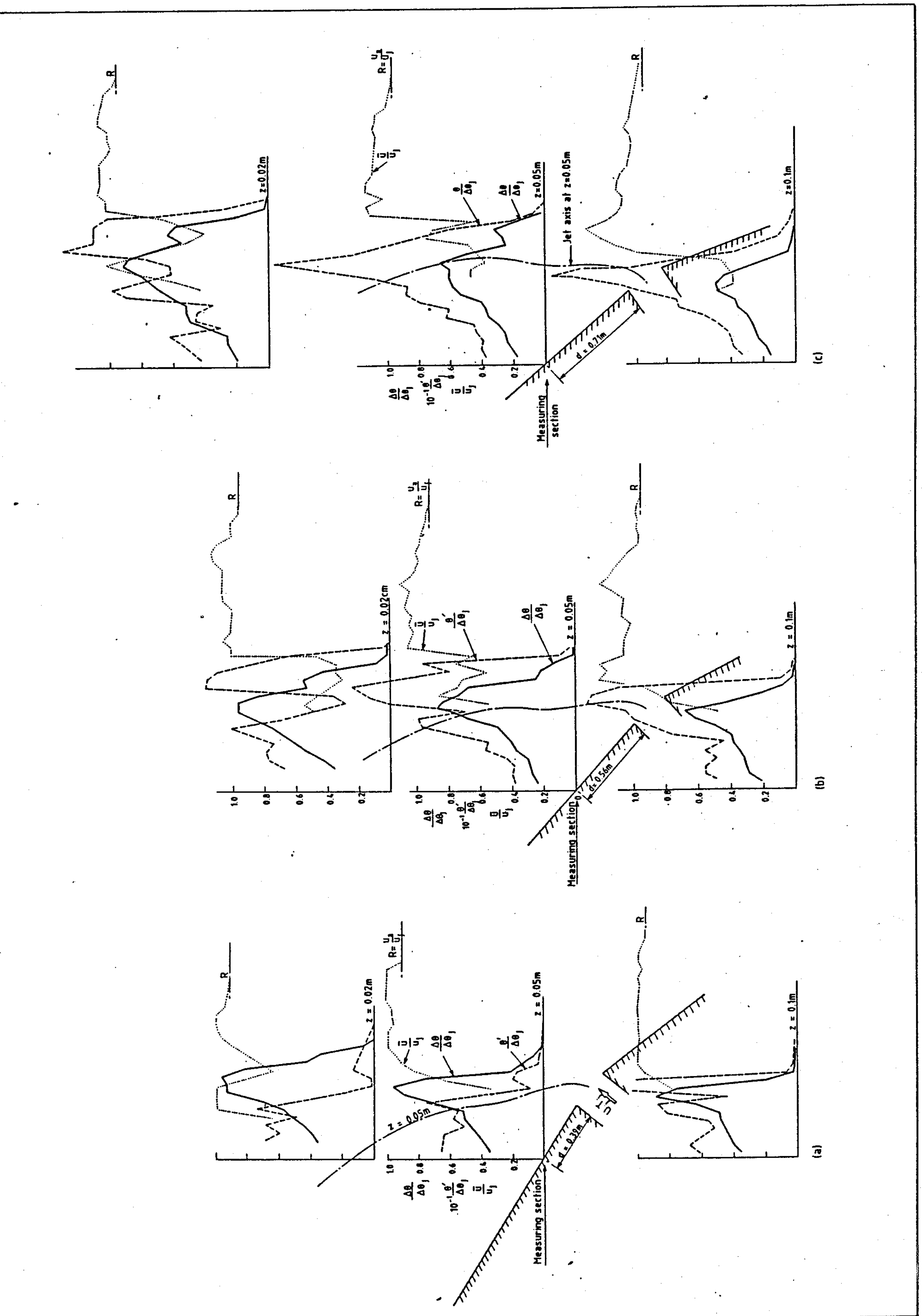

Fig 7 Lateral profiles of the mean velocity, mean temperature and temperature fluctuations at sections perpendicular to the jet-axis (a) at d = 0.39m, (b) at d = 0.56m and (c) at d = 0.71m

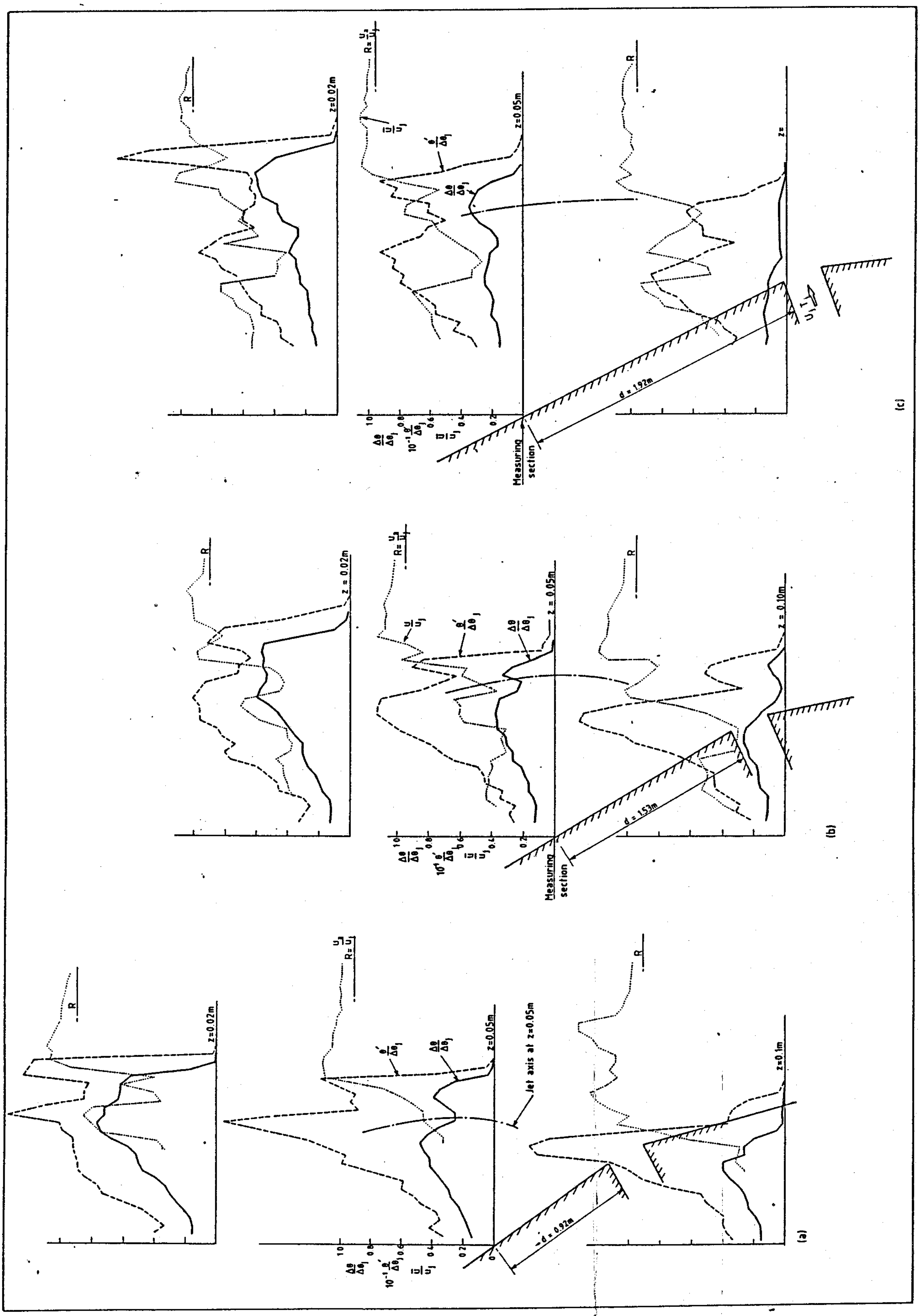

Fig 8 Lateral profiles of the mean velocity, mean temperature and temperature fluctuations at sections perpendicular to the jet-axis (a) at d = 0.92m, (b) at d = 1.53m and (c) at d = 1.92m

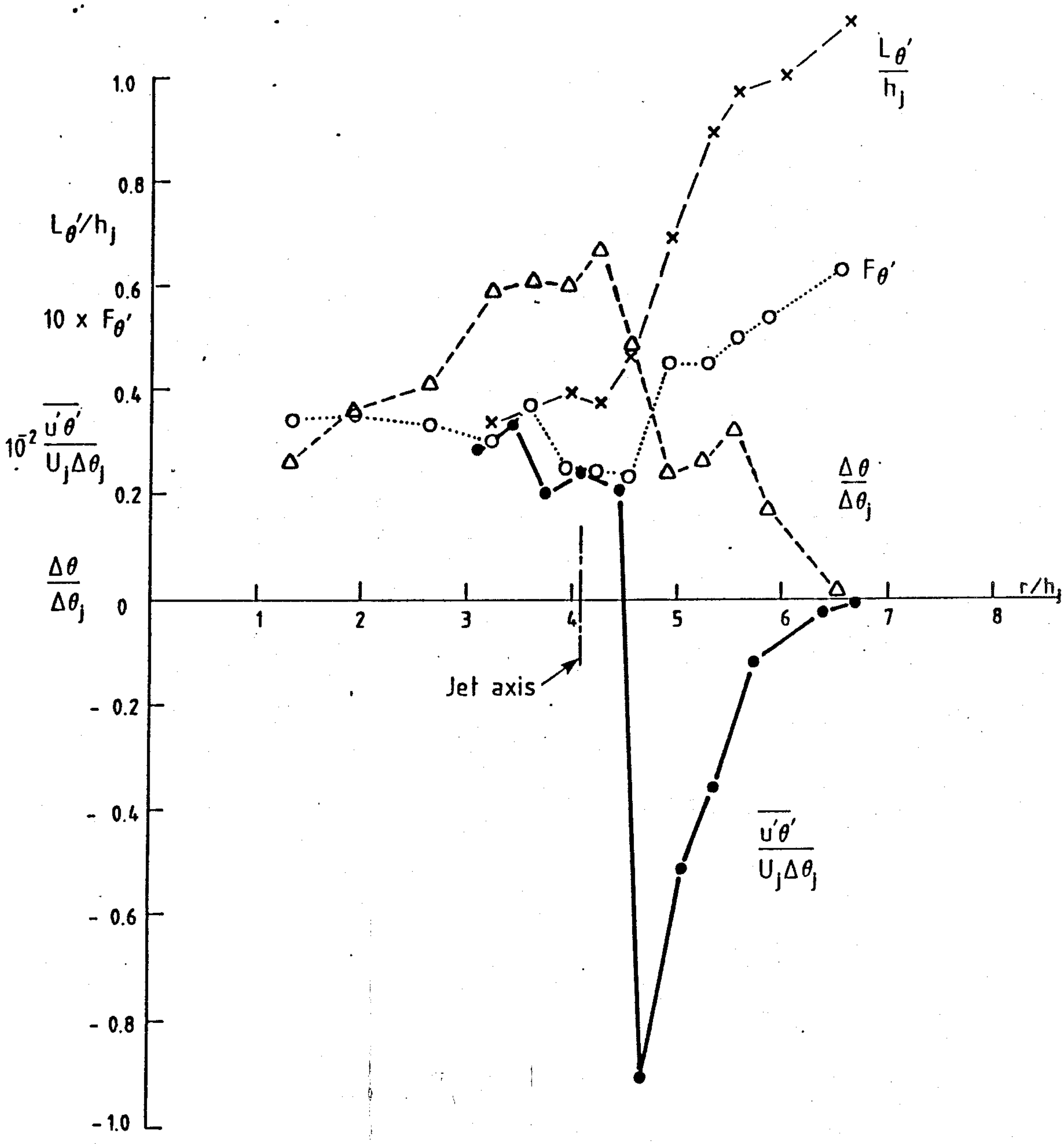

Fig 9 Lateral distribution of the turbulent warm water flux $\overline{u'\theta'}$, temperature flatness factor $F_{\theta'}$ and temperature length scale $L_{\theta'}$

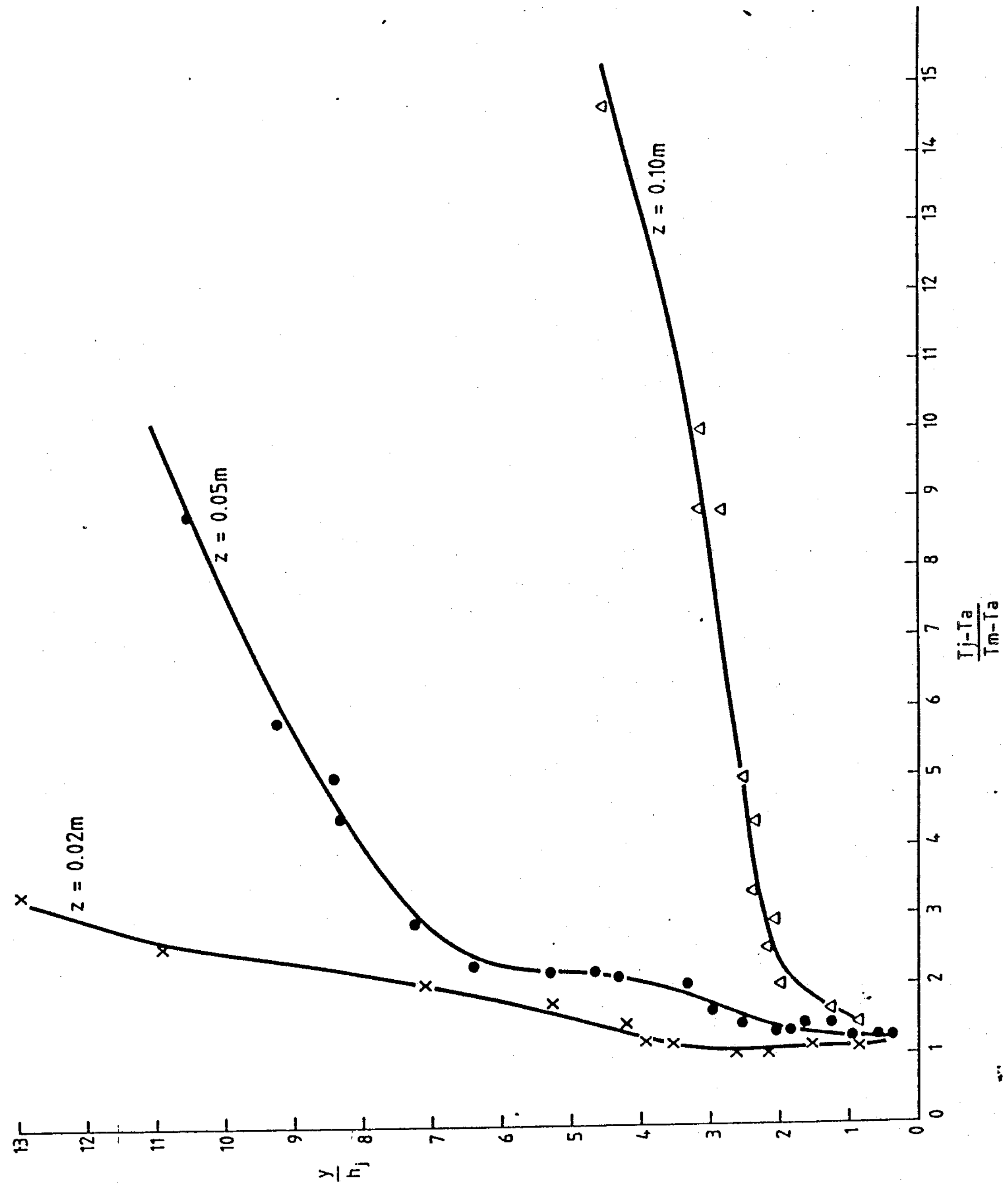

Fig 10 Dilution factor along the jet-axis at z = 0.02m, z = 0.05m and z = 0.10m below the free surface

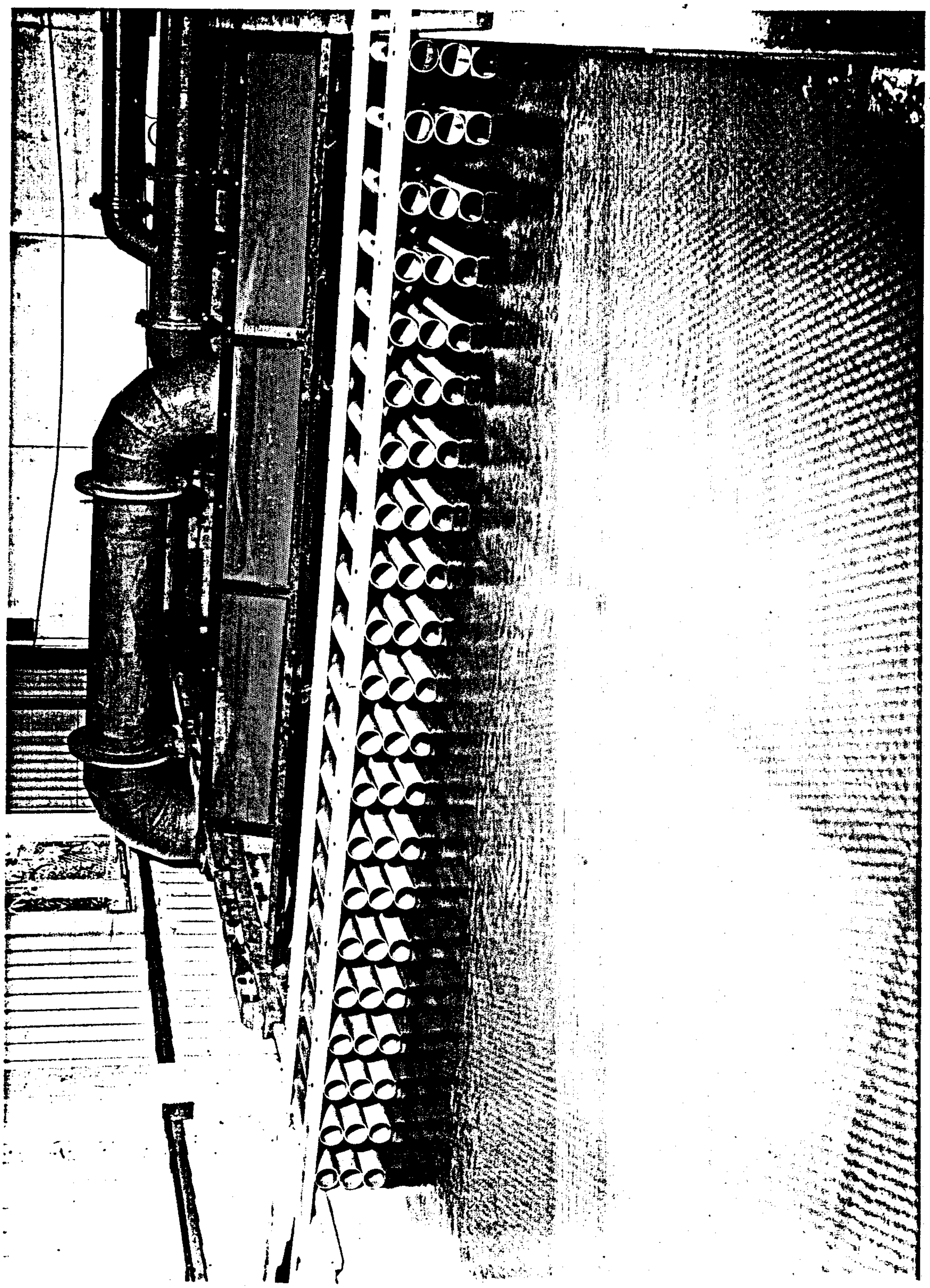

1 Cross-flow flume entrance arrangement and expanded mesh for tripping the flow

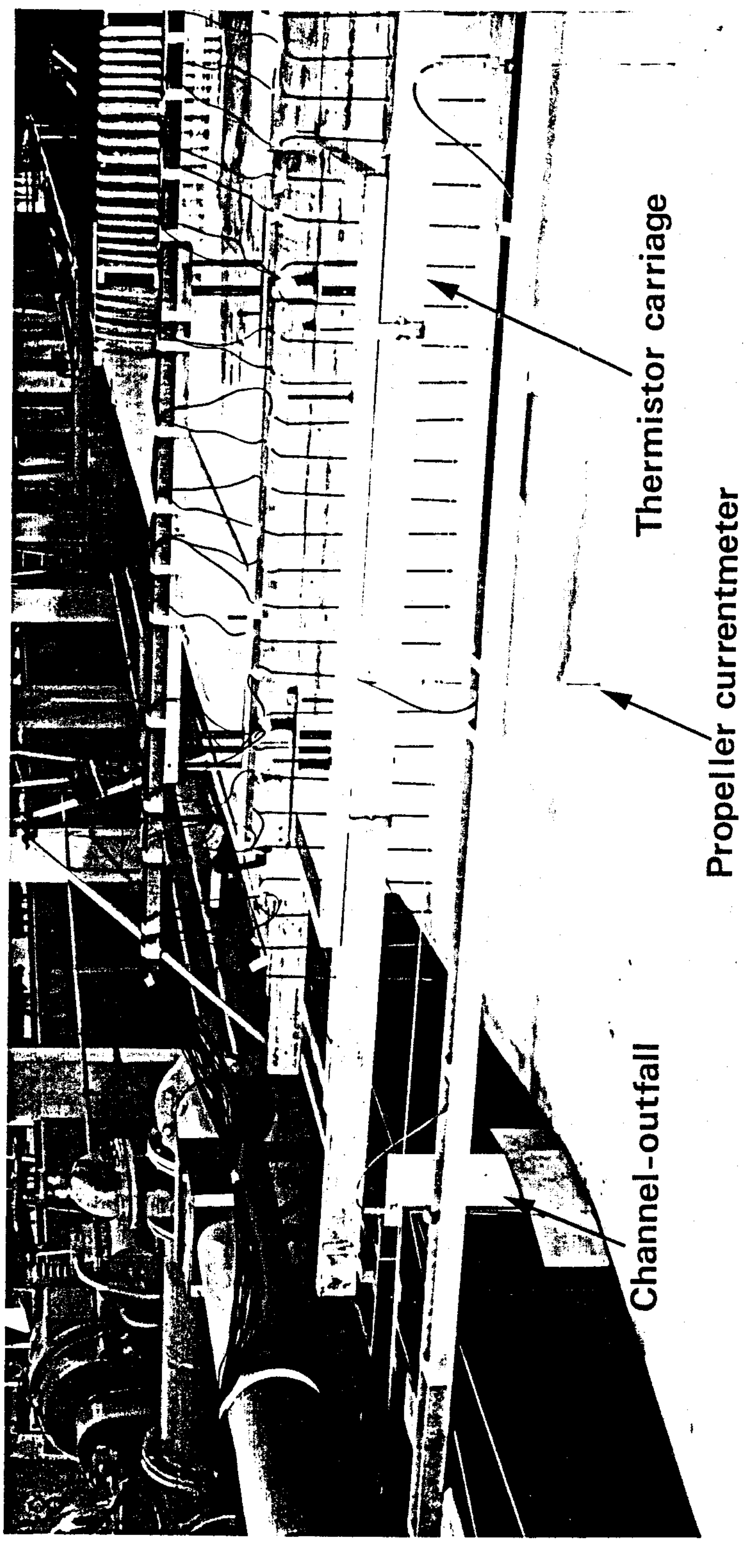

2 Channel outfall, thermistor frame and needle weirs

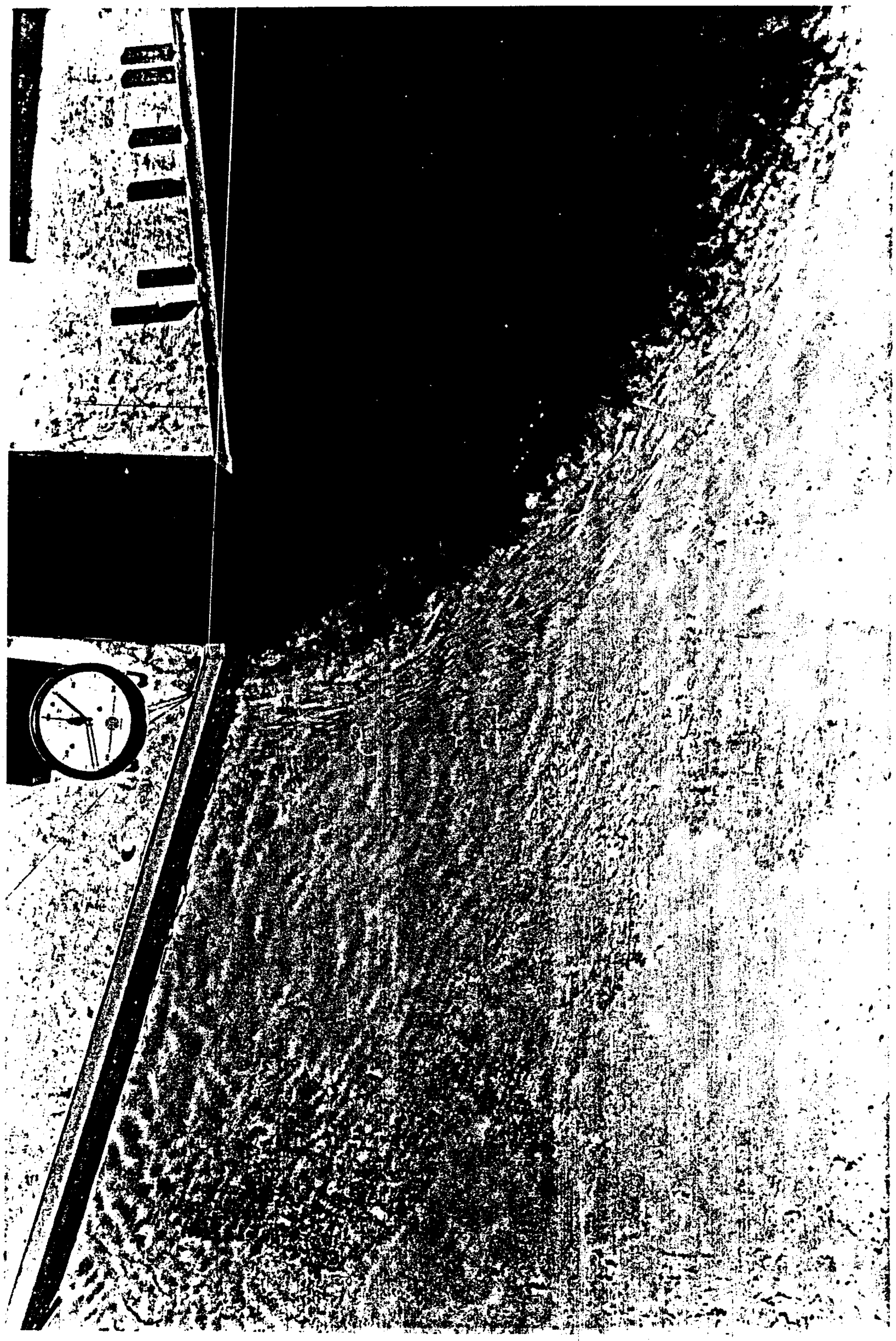

3 Spreading buoyant jet in a cross-flow with strong mixing in the outer edge